



Puzzling Variation of Gamma Rays from the Sun over the Solar Cycle Revealed with Fermi-LAT

A. Acharyya¹ , A. Adelfio², M. Ajello³ , L. Baldini^{4,5} , C. Bartolini^{6,7} , D. Bastieri^{8,9,10} , J. Becerra Gonzalez¹¹ , R. Bellazzini⁵ , B. Berenji¹², E. Bissaldi^{6,13} , R. D. Blandford¹⁴ , R. Bonino^{15,16} , E. Bottacini^{9,14}, S. Buson^{17,18} , R. A. Cameron¹⁴ , P. A. Caraveo¹⁹ , F. Casaburo^{20,21,22} , F. Casini²³, E. Cavazzuti²⁴ , D. Cerasole^{6,13}, N. Cibrario^{15,16}, S. Ciprini^{20,21} , G. Cozzolongo^{25,26} , P. Cristarella Orestano^{2,23} , F. Cuna⁶ , A. Cuoco^{15,16} , S. Cutini² , F. D'Ammando²⁷ , D. Depalo^{6,13}, S. W. Digel¹⁴ , N. Di Lalla¹⁴ , L. Di Venere⁶ , A. Domínguez²⁸ , A. Fiori²⁹ , Y. Fukazawa³⁰ , P. Fusco^{6,13} , F. Gargano⁶ , C. Gasbarra^{20,31} , D. Gasparrini^{20,21} , S. Germani^{2,32} , F. Giacchino^{20,21} , N. Giglietto^{6,13} , M. Giliberti^{6,13} , F. Giordano^{6,13} , M. Giroletti²⁷ , S. Guiriec^{33,34} , R. Gupta³⁴ , M. Hashizume³⁰ , E. Hays³⁴ , J. W. Hewitt³⁵ , A. Holzmann Airasca^{6,7} , D. Horan³⁶ , X. Hou³⁷ , T. Kayanoki³⁰ , M. Kuss⁵ , S. Larsson^{38,39} , A. Laviron^{34,40} , J. Li^{41,42} , A. Liguori^{6,13} , I. Liodakis⁴³ , P. Loizzo^{6,44} , F. Longo^{45,46} , F. Loparco^{6,13} , S. López Pérez³⁶ , L. Lorusso^{6,13} , M. N. Lovellette⁴⁷ , P. Lubrano² , S. Maldera¹⁵ , A. Manfreda⁵ , G. Martí-Devesa⁴⁵ , R. Martinelli^{45,46} , M. N. Mazziotta⁶ , J. E. McEnery^{45,46} , I. Mereu^{2,23} , M. Michailidis¹⁴ , P. F. Michelson¹⁴ , N. Mirabal^{34,49} , T. Mizuno⁵⁰ , P. Monti-Guarnieri^{45,46} , M. E. Monzani^{14,51} , A. Morselli²⁰ , I. V. Moskalenko¹⁴ , M. Negro⁵² , N. Omodei¹⁴ , E. Orlando^{14,45,46} , J. F. Ormes⁵³ , D. Paneque⁵⁴ , G. Panzarini^{6,13} , M. Persic^{46,55} , M. Pesce-Rollins⁵ , V. Petrosian¹⁴ , R. Pillera^{6,13} , G. Principe^{27,45,46} , S. Rainò^{6,13} , R. Rando^{8,9,10} , B. Rani^{34,49} , M. Razzano^{4,5} , A. Reimer⁵⁶ , O. Reimer⁵⁶ , M. Sánchez-Conde^{57,58} , P. M. Saz Parkinson⁵⁹ , D. Serini⁶ , C. Sgrò⁵ , E. J. Siskind⁶⁰ , P. Spinelli^{6,13} , D. Tak⁶¹ , L. Tibaldo⁶² , D. F. Torres^{63,64,65} , J. Valverde^{34,49} , Z. Wadiasingh^{34,48} , and W. Zhang^{64,65}

¹ Center for Cosmology and Particle Physics Phenomenology, University of Southern Denmark, Campusvej 55, DK-5230 Odense M, Denmark

² Istituto Nazionale di Fisica Nucleare, Sezione di Perugia, I-06123 Perugia, Italy

³ Department of Physics and Astronomy, Clemson University, Kinard Lab of Physics, Clemson, SC 29634-0978, USA

⁴ Università di Pisa, Dipartimento di Fisica E. Fermi, I-56127 Pisa, Italy

⁵ Istituto Nazionale di Fisica Nucleare, Sezione di Pisa, I-56127 Pisa, Italy

⁶ Istituto Nazionale di Fisica Nucleare, Sezione di Bari, I-70126 Bari, Italy; nicola.giglietto@ba.infn.it, silvia.raino@ba.infn.it

⁷ Università degli studi di Trento, via Calepina 14, 38122 Trento, Italy

⁸ Istituto Nazionale di Fisica Nucleare, Sezione di Padova, I-35131 Padova, Italy

⁹ Dipartimento di Fisica e Astronomia "G. Galilei," Università di Padova, Via F. Marzolo, 8, I-35131 Padova, Italy

¹⁰ Center for Space Studies and Activities "G. Colombo," University of Padova, Via Venezia 15, I-35131 Padova, Italy

¹¹ Instituto de Astrofísica de Canarias and Universidad de La Laguna, Dpto. Astrofísica, 38200 La Laguna, Tenerife, Spain

¹² California State University, Los Angeles, Department of Physics and Astronomy, Los Angeles, CA 90032, USA

¹³ Dipartimento di Fisica "M. Merlin" dell'Università e del Politecnico di Bari, via Amendola 173, I-70126 Bari, Italy

¹⁴ W. W. Hansen Experimental Physics Laboratory, Kavli Institute for Particle Astrophysics and Cosmology, Department of Physics and SLAC National Accelerator Laboratory, Stanford University, Stanford, CA 94305, USA; orland.ele@gmail.com

¹⁵ Istituto Nazionale di Fisica Nucleare, Sezione di Torino, I-10125 Torino, Italy

¹⁶ Dipartimento di Fisica, Università degli Studi di Torino, I-10125 Torino, Italy

¹⁷ Deutsches Elektronen Synchrotron DESY, D-15738 Zeuthen, Germany

¹⁸ Institut für Theoretische Physik and Astrophysik, Universität Würzburg, D-97074 Würzburg, Germany

¹⁹ INAF-Istituto di Astrofisica Spaziale e Fisica Cosmica Milano, via E. Bassini 15, I-20133 Milano, Italy

²⁰ Istituto Nazionale di Fisica Nucleare, Sezione di Roma "Tor Vergata," I-00133 Roma, Italy

²¹ Space Science Data Center - Agenzia Spaziale Italiana, Via del Politecnico, snc, I-00133, Roma, Italy

²² Dipartimento di Fisica, Università La Sapienza, Piazzale A. Moro, 2, I-00185 Roma, Italy

²³ Dipartimento di Fisica, Università degli Studi di Perugia, I-06123 Perugia, Italy

²⁴ Italian Space Agency, Via del Politecnico snc, 00133 Roma, Italy

²⁵ Friedrich-Alexander Universität Erlangen-Nürnberg, Erlangen Centre for Astroparticle Physics, Erwin-Rommel-Str. 1, 91058 Erlangen, Germany

²⁶ Friedrich-Alexander-Universität, Erlangen-Nürnberg, Schlossplatz 4, 91054 Erlangen, Germany

²⁷ INAF Istituto di Radioastronomia, I-40129 Bologna, Italy

²⁸ Grupo de Altas Energías, Universidad Complutense de Madrid, E-28040 Madrid, Spain

²⁹ Università di Pisa and Istituto Nazionale di Fisica Nucleare, Sezione di Pisa I-56127 Pisa, Italy

³⁰ Department of Physical Sciences, Hiroshima University, Higashi-Hiroshima, Hiroshima 739-8526, Japan

³¹ Dipartimento di Fisica, Università di Roma "Tor Vergata," I-00133 Roma, Italy

³² Dipartimento di Fisica e Geologia, Università degli Studi di Perugia, via Pascoli snc, I-06123 Perugia, Italy

³³ The George Washington University, Department of Physics, 725 21st St, NW, Washington, DC 20052, USA

³⁴ Astrophysics Science Division, NASA Goddard Space Flight Center, Greenbelt, MD 20771, USA

³⁵ University of North Florida, Department of Physics, 1 UNF Drive, Jacksonville, FL 32224, USA

³⁶ Laboratoire Leprince-Ringuet, CNRS/IN2P3, École polytechnique, Institut Polytechnique de Paris, 91120 Palaiseau, France

³⁷ Yunnan Observatories, Chinese Academy of Sciences, Kunming 650216, People's Republic of China

³⁸ Department of Physics, KTH Royal Institute of Technology, AlbaNova, SE-106 91 Stockholm, Sweden

³⁹ The Oskar Klein Centre for Cosmoparticle Physics, AlbaNova, SE-106 91 Stockholm, Sweden

⁴⁰ NASA Postdoctoral Program Fellow, USA

⁴¹ Department of Astronomy, University of Science and Technology of China, Hefei 230026, People's Republic of China

⁴² School of Astronomy and Space Science, University of Science and Technology of China, Hefei 230026, People's Republic of China

⁴³ Institute of Astrophysics, Foundation for Research and Technology-Hellas, Heraklion, GR-70013, Greece

⁴⁴ Dipartimento di Fisica dell'Università di Trento, via Sommarive, 14, Povo (TN), I-38123, Italy

⁴⁵ Dipartimento di Fisica, Università di Trieste, I-34127 Trieste, Italy

⁴⁶ Istituto Nazionale di Fisica Nucleare, Sezione di Trieste, I-34127 Trieste, Italy

- ⁴⁷ The Aerospace Corporation, 14745 Lee Rd, Chantilly, VA 20151, USA
- ⁴⁸ Department of Astronomy, University of Maryland, College Park, MD 20742, USA
- ⁴⁹ Center for Space Science and Technology, University of Maryland Baltimore County, 1000 Hilltop Circle, Baltimore, MD 21250, USA
- ⁵⁰ Hiroshima Astrophysical Science Center, Hiroshima University, Higashi-Hiroshima, Hiroshima 739-8526, Japan
- ⁵¹ Vatican Observatory, Castel Gandolfo, V-00120, Vatican City State
- ⁵² Department of physics and Astronomy, Louisiana State University, Baton Rouge, LA 70803, USA
- ⁵³ Department of Physics and Astronomy, University of Denver, Denver, CO 80208, USA
- ⁵⁴ Max-Planck-Institut für Physik, D-80805 München, Germany
- ⁵⁵ INAF-Astronomical Observatory of Padova, Vicolo dell'Osservatorio 5, I-35122 Padova, Italy
- ⁵⁶ Institut für Astro- und Teilchenphysik, Leopold-Franzens-Universität Innsbruck, A-6020 Innsbruck, Austria
- ⁵⁷ Instituto de Física Teórica UAM/CSIC, Universidad Autónoma de Madrid, E-28049 Madrid, Spain
- ⁵⁸ Departamento de Física Teórica, Universidad Autónoma de Madrid, 28049 Madrid, Spain
- ⁵⁹ Santa Cruz Institute for Particle Physics, Department of Physics and Department of Astronomy and Astrophysics, University of California at Santa Cruz, Santa Cruz, CA 95064, USA
- ⁶⁰ NYCB Real-Time Computing Inc., Lattintown, NY 11560-1025, USA
- ⁶¹ SNU Astronomy Research Center, Seoul National University, Seoul 08826, Republic of Korea
- ⁶² IRAP, Université de Toulouse, CNRS, UPS, CNES, F-31028 Toulouse, France
- ⁶³ Institució Catalana de Recerca i Estudis Avançats (ICREA), E-08010 Barcelona, Spain
- ⁶⁴ Institute of Space Sciences (ICE, CSIC), Campus UAB, Carrer de Magrans s/n, E-08193 Barcelona, Spain
- ⁶⁵ Institut d'Estudis Espacials de Catalunya (IEEC), E-08034 Barcelona, Spain
- Received 2025 May 9; revised 2025 June 25; accepted 2025 July 11; published 2025 August 7

Abstract

The steady-state gamma-ray emission from the Sun is thought to consist of two emission components due to interactions with Galactic cosmic rays: (1) a hadronic disk component, and (2) a leptonic extended component peaking at the solar edge and extending into the heliosphere. The flux of these components is expected to vary with the 11 yr solar cycle, being highest during solar minimum and lowest during solar maximum, as it varies with the cosmic-ray flux. No study has yet analyzed the flux variation of each component over solar cycles. In this work, we measure the temporal variations of the flux of each component over 15 yr of Fermi Large Area Telescope observations and compare them with the sunspot number and Galactic cosmic-ray flux from AMS-02 near Earth. We find that the flux variation of the disk anticorrelates with the sunspot number and correlates with cosmic-ray protons, as expected, confirming its emission mechanism. In contrast, the extended component exhibits a more complex variation: despite an initial anticorrelation with the sunspot number, we find neither anticorrelation with the sunspot number nor correlation with cosmic-ray electrons over the full 15 yr period. This most likely suggests that cosmic-ray transport and modulation in the inner heliosphere are unexpectedly complex and may differ for electrons and protons or, alternatively, that there is an additional, unknown component of gamma rays or cosmic rays. These findings impact space weather research and emphasize the need for close monitoring of Cycle 25 and the ongoing polarity reversal.

Unified Astronomy Thesaurus concepts: [Quiet sun \(1322\)](#); [Gamma-rays \(637\)](#); [Cosmic rays \(329\)](#)

1. Introduction

Over the last 15 yr, the Sun has been observed to be a gamma-ray source in its quiet state (E. Orlando & A. W. Strong 2008), i.e., in its nonflaring state or nonflaring regions. H. S. Hudson (1989) and D. Seckel et al. (1991) made the first calculations of the gamma-ray emission from pion decay by Galactic cosmic-ray (CR) cascades in the solar atmosphere. This emission was expected to be confined to the region of the solar disk. The flux was expected to vary during the solar cycle, as observed for the lunar gamma-ray flux (D. J. Thompson et al. 1997), which is produced by similar mechanisms. The existence of a spatially extended inverse Compton (IC) component from scattering by CR electrons on solar photons was theorized by I. V. Moskalenko et al. (2006) and E. Orlando & A. W. Strong (2007) independently. This broad emission was expected to be brighter at the solar edges and roughly inversely proportional to the angular distance from the Sun, as recently confirmed by refined IC models (E. Orlando & A. Strong 2021). Recent theoretical studies

have also focused on improving models of the disk component (e.g., B. Zhou et al. 2017; C. Niblaeus et al. 2019; J. Becker Tjus et al. 2020; M. Gutiérrez & M. Masip 2020; H. S. Hudson et al. 2020; M. N. Mazziotta et al. 2020; J.-T. Li et al. 2024; Z. Li et al. 2024).

Due to their association with CRs, the intensity of both the disk and extended components of the gamma-ray emission from the quiet Sun is predicted to vary over the solar cycle and, in particular, to anticorrelate with the sunspot number (SSN) and to correlate with the CR flux as measured near Earth.

The first evidence of the gamma-ray emission from the quiet Sun was found by E. Orlando & A. W. Strong (2008) by analyzing the entire archival EGRET data. However, the limited sensitivity of EGRET precluded the investigation of flux variation over time. The launch of the Fermi Gamma-Ray Space Telescope in 2008 enabled observations of the quiet Sun with high statistical significance. Observations of solar emission during the first 18 months of the Fermi Large Area Telescope (LAT) mission, a time period during solar minimum, were reported in A. A. Abdo et al. (2011) and were in agreement with E. Orlando & A. W. Strong (2008). Variations of the solar flux with solar activity were first reported by K. C. Y. Ng et al. (2016) with 6 yr of Fermi-LAT



Original content from this work may be used under the terms of the [Creative Commons Attribution 4.0 licence](#). Any further distribution of this work must maintain attribution to the author(s) and the title of the work, journal citation and DOI.

observations. They found the gamma-ray flux of the solar emission to be larger during solar minimum than during solar maximum. More recent works (Q.-W. Tang et al. 2018; T. Linden et al. 2022) updated the analysis over almost the entire 11 yr cycle and found that the solar flux varies by nearly a factor of 2 between the solar maximum and the solar minimum. Moreover, T. Linden et al. (2022) found that the variation in the 0.1–10 GeV range is not dependent on energy, differing from what was expected. More recent observations with HAWC (A. Albert et al. 2023) showed the solar flux extending to TeV energies during solar minimum, and an upper limit during solar maximum was observed.

In summary, the observed solar gamma-ray flux variations have confirmed a trend of anticorrelation with the solar activity. However, the extended IC component has not been included in these studies. Hence, contamination of the disk flux measurement by the extended component is not excluded in previous works. To date, no studies have examined the correlation of the two distinct components with CR proton and electron fluxes, or their anticorrelation with solar activity. In this Letter, we report results for 15 yr of Fermi-LAT observations of the Sun, allowing us to distinguish the two solar components and to study their flux variations over Solar Cycle 24 and the first years of Solar Cycle 25.

2. Method

We use observations with Fermi-LAT (W. B. Atwood et al. 2009), which detects gamma rays from 20 MeV to over 300 GeV. In survey mode, the LAT observes the full sky approximately every 3 hr with an almost uniform daily exposure. This capability, combined with its large field of view of 2.4 sr (at 1 GeV) and high sensitivity, allows us to observe the Sun daily.

2.1. Data Selection

We analyze 15 yr of Fermi-LAT observations, specifically from 2008 August 4 to 2023 June 30 in the 70 MeV–70 GeV energy range. We select the Pass 8 SOURCE event class (W. Atwood et al. 2013; P. Bruel et al. 2018) and P8R3_SOURCE_V6 instrument response functions,⁶⁶ and excluded times when the LAT was within the South Atlantic anomaly. To reduce contamination from CR interactions with the upper atmosphere, events with zenith angles larger than 90° are excluded. Because the Sun is moving across the sky, the analysis of its emission requires special handling. In addition to the standard Fermi-LAT Science Tools package,⁶⁷ dedicated tools are used where data are selected in a moving frame centered on the instantaneous position of the Sun, which is computed using an interface to the JPL ephemeris libraries.⁶⁸ As in A. A. Abdo et al. (2011), to further reduce contamination while maintaining useful data, we apply a carefully customized selection: data are excluded when the Sun is within 30° of the Galactic plane, 20° of the Moon, and 10° of the four bright sources along its path (3C 454.3, PSR J1620–4927, Geminga, and the Crab Nebula). In addition, all solar flares listed in the LAT Solar Flare Catalog (M. Ajello

et al. 2021) are removed. Also, to remove any contamination from fainter solar flares and other flaring or bright sources close to the path of the Sun, in this work, we develop a dedicated procedure involving the monitoring of light curves in nested regions centered on the Sun. After inspection, we remove the time intervals when short variations of light-curve fluxes exceed 5σ from the average flux value, using 3 hr time bins. These cuts produce a very clean event sample by removing about 55% data in total.

2.2. Background Evaluation

After applying our data cuts, there may still be possible contamination in the region around the Sun from diffuse Galactic and isotropic gamma-ray emissions, as well as from weak point sources along the ecliptic. This contamination is referred to as background. Correct evaluation of the background is essential for analyzing solar emission, as IC emission extends beyond 20° from the Sun (E. Orlando & A. W. Strong 2007).

As in A. A. Abdo et al. (2011), we determine the background by applying the off-source (or “fake” source) method: an imaginary source follows the path of the Sun along the ecliptic but at a different time, which means at a different distance from the real Sun. The data sample we use for the background determination is centered on the off-source position and has the same selection cuts applied to the data sample of the Sun. For a careful evaluation of the background, we compute seven fake sources from 90° to 270° from the Sun in steps of 30°. Moreover, we divide the 15 yr data set into 2 yr subsamples, each starting six months after the previous one, on which we perform the binned maximum likelihood technique as described by J. R. Mattox et al. (1996), using glike as included in the FermiTools. We do it by iteratively adjusting the energy spectrum in order to maximize the likelihood of the data given the model. We find the seven background fluxes to be within $\pm 3\%$ of their average values. Following A. A. Abdo et al. (2011), this 3% variation defines the systematic uncertainty on the solar components. Then, we use the output of the likelihood analysis for each time interval as the background model for the corresponding data set centered on the Sun.

2.3. Analysis of the Solar Components

We evaluate the gamma-ray flux variation over time by dividing the 15 yr data set into 2 yr subsamples, each starting six months after the previous one, similar to the procedure for the background. For the binned maximum likelihood analysis, we use a bin size of 0.1 and the energy dispersion ($\text{edisp_bins} = -2$). Three components are considered simultaneously in the analysis: the solar disk component, the solar extended component, and the background. The latter is fixed as previously described and masked over the solar disk. We model the disk with emission confined within a radius of 0.265 from the solar center, corresponding to the average radius of the Sun. We model the extended component with emission starting from the edge of the solar disk and decreasing inversely with the elongation angle from the Sun, following solar IC emission models (E. Orlando & A. W. Strong 2007, 2008; E. Orlando & A. Strong 2021), as in A. A. Abdo et al. (2011). Both energy spectra are modeled with a log-parabolic function. The solar model components are

⁶⁶ P8R3 data do not contain the residual background events near the ecliptic present in P8R2, which could have affected the analysis.

⁶⁷ FermiTools version 2.2.0, <https://fermi.gsfc.nasa.gov/ssc/data/analysis/software/>.

⁶⁸ <https://ssd.jpl.nasa.gov/horizons/>

convolved with the energy-dependent point-spread function, while the background component is not, because it is derived from observational data.

3. Temporal Variation Results

The two components are clearly separately measured⁶⁹ and their flux variations are integrated over 2 yr subsamples. Then, the disk and extended component variations are compared with the flux of CR protons (M. Aguilar et al. 2021) and CR electrons (M. Aguilar et al. 2023), respectively, and with the SSN.⁷⁰

The correlation between these data sets (solar flux, CR flux, and SSN) is visually inspected and statistically investigated by calculating the Pearson correlation coefficient (K. F. R. S. Pearson 1920; E. S. Pearson 1931, 1932) and the z -transformed discrete correlation function (zDCF;⁷¹ R. D. Blandford & C. F. McKee 1982; R. A. Edelson & J. H. Krolik 1988; T. Alexander 2013). The eventual time lag between data sets is also evaluated. For a proper correlation study, the data sets of Fermi-LAT, the daily CR fluxes, and the monthly SSN are interpolated or averaged over the same time bin of 30 days. We test the robustness of the results using nonoverlapping 2 yr subsamples, each starting six months after the previous one, to verify that the results are not sensitive to the choice of subsample start times. Since solar flux variations in subsamples are integrated over 2 yr periods starting every six months, an apparent trend on a timescale shorter than 2 yr should not be interpreted as physically meaningful.

The results for the two components are reported below.

3.1. Disk Component

Figure 1 shows details of the disk emission. Panel (a) shows the flux variation expressed as a fraction of the average flux of the disk component for energies greater than 250 MeV, 500 MeV, and 1 GeV over time. The regions with different shades of gray represent the systematic uncertainties. The variations in the three integral energy ranges are synchronous, and the variation of the disk flux with the solar cycle is clearly demonstrated. For all three energy ranges, the disk flux varies by $\pm 40\%$ with respect to the average value. Panel (b) shows the anticorrelation between the disk flux variation above 1 GeV and the SSN over time. This is consistent with expectations, as CR-induced emission is expected to vary over the solar cycle in anticorrelation with solar activity (e.g., D. J. Thompson et al. 1997; K. C. Y. Ng et al. 2016). Panel (c) shows the correlation between the disk flux variation above 1 GeV and the temporal variation of the CR proton flux at ~ 2 GeV as observed by AMS-02. Hence, the hadronic emission of the disk component around GeV energies is correctly identified. This also means that the modulation of CR protons at Earth is temporally coincident with the modulation at the Sun within the 2 yr resolution of the gamma-ray fluxes. Panel (d) shows the correlation between the solar disk flux above 1 GeV and the lunar flux (M. Ackermann et al. 2016).

⁶⁹ The significance of the detection of each component is verified for each data point, being the test statistic > 300 .

⁷⁰ SSN data are downloaded from the World Data Center SILSO, https://www.sidc.be/SILSO/DATA/SN_ms_tot_V2.0.txt.

⁷¹ Because the Pearson coefficient may not be accurate for nonlinear relationships (G. U. Yule 1926; J. D. Scargle 2020; P. M. Riechers & J. P. Crutchfield 2021), we also use zDCF, which is better suited for temporal cross-correlations and commonly applied to nonlinear cases.

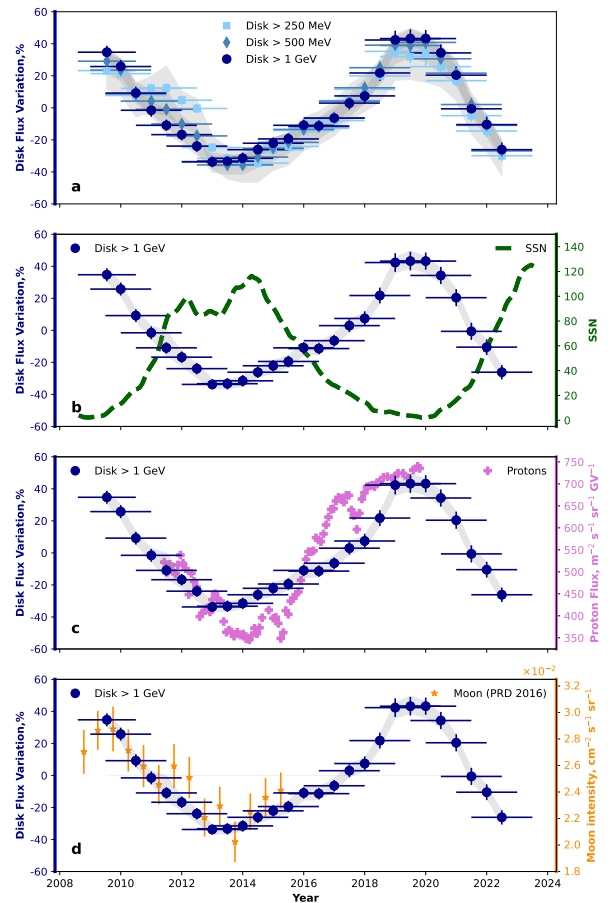


Figure 1. Panel (a): percentage of the flux variation of the solar disk component above 25 MeV, 500 MeV, and 1 GeV vs. time in years. For normalization, the average flux values used are 9.15, 4.69, and $2.23 \times 10^{-8} \text{ cm}^{-2} \text{ s}^{-1}$, respectively. The gray regions define systematic uncertainties. Panel (b): flux variation in time of the solar disk component above 1 GeV compared with the SSN. Panel (c): flux variation in time of the solar disk component above 1 GeV compared with the CR proton flux at 2.14–2.4 GV (M. Aguilar et al. 2021). Panel (d): flux variation in time of the solar disk component above 1 GeV compared with the Moon’s flux above 56 MeV (M. Ackermann et al. 2016).

The lunar flux variations throughout the period (F. Loparco et al. 2025, in preparation) show a similar trend. This corroborates the theory that both solar disk and lunar emission share a similar production mechanism. The comparisons in panels (b), (c), and (d) give Pearson and zDCF correlations (or anticorrelations) above 0.9⁷² with no significant time lag.

3.2. Spatially Extended Component

Figure 2 shows details of the extended component. Panel (a) shows the flux variation expressed as a fraction of the average flux of the solar extended component for energies greater than 250 MeV, 500 MeV, and 1 GeV over time. The gray-shaded regions represent its systematic uncertainties. For the three integral energy ranges, the flux varies by $+40\%$ and -60% between its maximum and minimum values. In comparison to the disk emission, the systematic errors for the extended component are larger due to the uncertainties in the background estimation.

⁷² We find this value for the nonoverlapping 2 yr subsamples, and also for all data points.

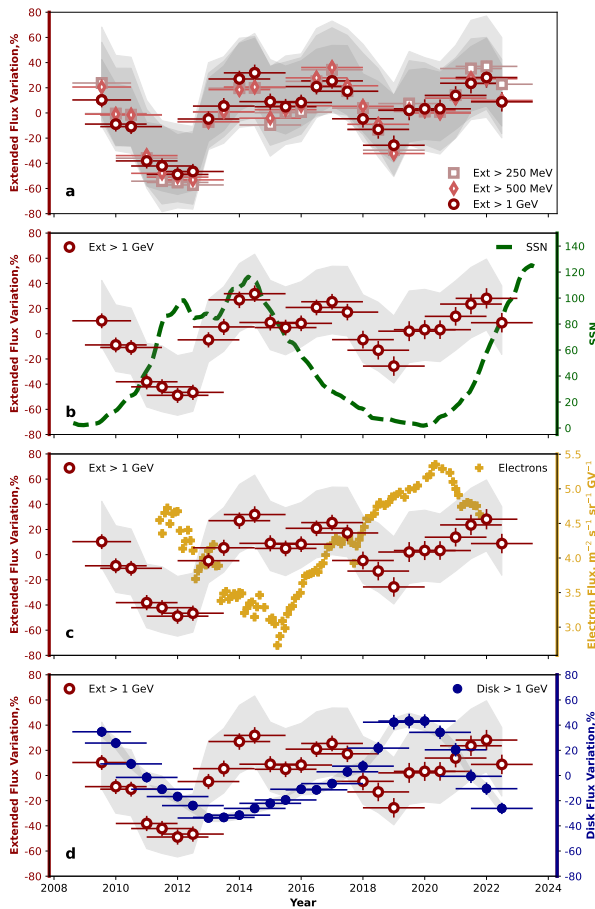


Figure 2. Panel (a): percentage of the flux variation of the solar extended component above 250 MeV, 500 MeV, and 1 GeV vs. time. For normalization, the average flux values used are 30.00, 13.99, and 5.95 ($\times 10^{-8} \text{ cm}^{-2} \text{ s}^{-1}$), respectively. The gray region defines systematic uncertainties. Panel (b): flux variation of the solar extended component above 1 GeV compared with the SSN. Panel (c): flux variation of the solar extended component above 1 GeV compared with the CR electron flux at 1.00–1.71 GV (M. Aguilar et al. 2023). Panel (d): flux variation of the solar extended component above 1 GeV compared with the flux variation of the disk component above 1 GeV.

The extended flux variation above 1 GeV is compared with the SSN (panel (b) of the same figure) and with the temporal variation of the CR electron⁷³ flux at 1 GeV as observed by AMS-02 (panel (c)). The plots show a complex relationship between the extended component flux variation and both the SSN and CR electron flux. Indeed, the correlation coefficients over the entire period are below 0.3, indicating no significant correlation. Because the periods before 2011 lack CR electron measurements from AMS-02, to gain insights into this complex trend of the extended component, panel (d) shows a temporal comparison between the flux variations of the extended component and the disk. A visual comparison of panels (b), (c), and (d) appears to reveal periods consistent with expectations, as well as periods contrary to them. The correlation coefficients with the disk flux variation and the SSN, calculated only for the period from 2008 August to 2012 July, show strong correlation and anticorrelation (above 0.9), respectively, in line with expectations.

⁷³ The IC component also includes positrons, but their flux accounts for at most a few percent of the total.

4. Discussion and Conclusions

We report for the first time the temporal variation of the flux of both distinct gamma-ray components of the solar emission over 15 yr of Fermi-LAT observations. In the following, we discuss the two solar emission components separately.

The flux variation in time of the disk anticorrelates with the SSN and correlates with CR protons, confirming its emission mechanism. It generally agrees with the results of T. Linden et al. (2022) obtained for a shorter period. Possible differences are attributable to different temporal binning and data selections. Interestingly, we find that the variation in time is independent of energy above 250 MeV, whereas the flux in the lowest energy range is expected to vary the most⁷⁴ due to the stronger modulation of CRs at lower energies. The fact that the relative variation of fluxes does not depend on energy was already anticipated by T. Linden et al. (2022). It can be an indication that the solar magnetic field plays an important role in the variability, as the intricate structure of the field at the Sun would lead to complex energy and time variations.

The variation of the extended component has not been investigated before.⁷⁵ We find temporal anticorrelation between the extended flux variation and the SSN from 2008 August to 2012 June, and correlation between the extended flux variation and the disk variation over the same period. However, for 2013–2023, we no longer observe any correlation/anticorrelation, not even with the CR electron flux. Similarly to the disk, the variation is independent of energy.

The variations of the extended component come as a surprise and challenge current theoretical models and assumptions. We do not provide a definitive interpretation of these results; instead, we highlight related observational and modeling challenges to illustrate the complexity of the topic. For example, in the outer heliosphere, it has long been accepted that CR electrons are modulated similarly to protons (e.g., L. J. Gleeson & W. I. Axford 1968) and that their modulation anticorrelates with the SSN. However, several studies on heliospheric CR propagation beyond 1 au have reported indications, based on measurements (e.g., M. Aguilar et al. 2018) and models (e.g., M. S. Potgieter 2013; M. S. Potgieter & E. E. Vos 2017; N. Tomassetti et al. 2017, 2022; R. A. Caballero-Lopez et al. 2019), that CR modulation and propagation depend on the particle’s charge sign and the solar magnetic polarity. For protons, N. Tomassetti et al. (2017) proposed a simple predictive model of solar modulation in the outer heliosphere that depends on the SSN and the tilt angle to explain the observed time lag between solar activity data and CR measurements. This time lag is found to depend on the solar polarity. Recently, in order to explain the modulation over time of the AMS-02 CR electrons, O. P. M. Aslam et al. (2023) calculated that particle drift in the outer heliosphere becomes negligible during the period when the polarity is not well defined and starts recovering just after the polarity reversal, but the mean free path keeps decreasing or remains unchanged for some period after the polarity reversal. On the other hand, the propagation of CR electrons, in the inner heliosphere, i.e., within 1 au of the Sun, has received comparatively little attention. A recent study on CR transport

⁷⁴ Calculations in M. N. Mazziotta et al. (2020) around solar maximum might suggest weak energy independence, though this remains speculative due to limited coverage and the absence of calculations during solar minimum.

⁷⁵ After completing this work and the manuscript, we became aware of a related study by T. Linden et al. (2025), which had just appeared on arXiv.

in the inner heliosphere (V. Petrosian et al. 2023) shows that electrons undergo multiple scattering due to turbulence and experience significant energy losses as they approach the Sun. Based on this, we expect that at higher energies, the reduced electron flux near the Sun under stronger magnetic fields would decrease the IC emission, reinforcing the expected anticorrelation with solar activity.

While most of the current literature focuses on CR propagation in the outer heliosphere rather than in the inner heliosphere, our present results suggest that the details of CR electron transport and modulation in the inner heliosphere are even more complex than in the outer heliosphere. Hence, models of CR electron propagation that work beyond 1 au may not be extrapolated down to the Sun. Modulation and propagation within 1 au of the Sun have rarely been studied because of poor observational constraints. Our work can shed light on the propagation of CRs in the inner Galaxy through the study of the variation of the CR-induced emission from the Sun.

Curiously, at the end of 2012, the reversal of the Sun's polar magnetic field began, which resulted in the change of polarity in Cycle 24. Concurrently with the reversal, unexplained asymmetric emission from the Sun in the GeV range has recently been observed (B. Arsioli & E. Orlando 2024). Interestingly, the polarity reversal was unusual (P. Janardhan et al. 2018; L. A. Upton & D. H. Hathaway 2023) with the south polarity flipping in 2013, while the north polarity being delayed to the end of 2014.

Our results also suggest, as do other studies (e.g., T. Linden et al. 2018; Q.-W. Tang et al. 2018), a possible crucial role of the solar magnetic field, which remains unexplained. Possibly, CR electron transport and modulation models in the inner heliosphere may be constrained by observations of synchrotron radiation in X-rays produced by these electrons interacting with the solar magnetic field, as recently theorized by E. Orlando et al. (2023). Other effects may also play an important role (e.g., K. C. Y. Ng et al. 2024; E. Puzzoni et al. 2024; M. N. Mazziotta 2025).

Our results may even call into question whether the spatially extended emission is produced mainly by Galactic CR electrons. This may potentially include an unknown additional mechanism of gamma-ray production or an additional component of high-energy CR close to the Sun. Both hypotheses would need to be investigated further.

To conclude, the discovery reported in this work presents an additional challenge to our understanding of the Sun in gamma rays. This adds to the detection of the solar unexplained spectral dip (T. Linden et al. 2018), the observations of an unexpected asymmetry in GeV emission from the disk (B. Arsioli & E. Orlando 2024), and the detection of GeV and TeV solar emission at higher energies than expected (A. A. Abdo et al. 2011; T. Linden et al. 2018; A. Albert et al. 2023). A revision of current models and timely observations of CRs and the Sun during the current Cycle 25, as well as during the reversal in polarity, all will help in understanding the unexpected trend of the solar extended emission and its relation to the solar cycles.




Acknowledgments

The Fermi-LAT Collaboration acknowledges generous ongoing support from a number of agencies and institutes that have supported both the development and the operation of the

LAT as well as scientific data analysis. These include the National Aeronautics and Space Administration and the Department of Energy in the United States, the Commissariat à l'Énergie Atomique and the Centre National de la Recherche Scientifique / Institut National de Physique Nucléaire et de Physique des Particules in France, the Agenzia Spaziale Italiana and the Istituto Nazionale di Fisica Nucleare in Italy, the Ministry of Education, Culture, Sports, Science and Technology (MEXT), High Energy Accelerator Research Organization (KEK) and Japan Aerospace Exploration Agency (JAXA) in Japan, and the K. A. Wallenberg Foundation, the Swedish Research Council and the Swedish National Space Board in Sweden. Additional support for science analysis during the operations phase is gratefully acknowledged from the Istituto Nazionale di Astrofisica in Italy and the Centre National d'Études Spatiales in France. This work was performed, in part, under DOE Contract DE-AC02-76SF00515. Also, partial support from NASA grant Nos. 80NSSC20K1558 and 80NSSC22K0495 is acknowledged.

ORCID iDs

- A. Acharyya  <https://orcid.org/0000-0002-2028-9230>
M. Ajello  <https://orcid.org/0000-0002-6584-1703>
L. Baldini  <https://orcid.org/0000-0002-9785-7726>
C. Bartolini  <https://orcid.org/0000-0001-7233-9546>
D. Bastieri  <https://orcid.org/0000-0002-6954-8862>
J. Becerra Gonzalez  <https://orcid.org/0000-0002-6729-9022>
R. Bellazzini  <https://orcid.org/0000-0002-2469-7063>
E. Bissaldi  <https://orcid.org/0000-0001-9935-8106>
R. D. Blandford  <https://orcid.org/0000-0002-1854-5506>
R. Bonino  <https://orcid.org/0000-0002-4264-1215>
S. Buson  <https://orcid.org/0000-0002-3308-324X>
R. A. Cameron  <https://orcid.org/0000-0003-0942-2747>
P. A. Caraveo  <https://orcid.org/0000-0003-2478-8018>
F. Casaburo  <https://orcid.org/0000-0002-2260-9322>
E. Cavazzuti  <https://orcid.org/0000-0001-7150-9638>
S. Ciprini  <https://orcid.org/0000-0002-0712-2479>
G. Cozzolongo  <https://orcid.org/0009-0001-3324-0292>
P. Cristarella Orestano  <https://orcid.org/0000-0003-3219-608X>
F. Cuna  <https://orcid.org/0000-0003-3414-9092>
A. Cuoco  <https://orcid.org/0000-0003-1504-894X>
S. Cutini  <https://orcid.org/0000-0002-1271-2924>
F. D'Ammando  <https://orcid.org/0000-0001-7618-7527>
S. W. Digel  <https://orcid.org/0000-0002-5296-4720>
N. Di Lalla  <https://orcid.org/0000-0002-7574-1298>
L. Di Venere  <https://orcid.org/0000-0003-0703-824X>
A. Domínguez  <https://orcid.org/0000-0002-3433-4610>
A. Fiori  <https://orcid.org/0000-0003-3174-0688>
Y. Fukazawa  <https://orcid.org/0000-0002-0921-8837>
P. Fusco  <https://orcid.org/0000-0002-9383-2425>
F. Gargano  <https://orcid.org/0000-0002-5055-6395>
C. Gasbarra  <https://orcid.org/0000-0001-8335-9614>
D. Gasparrini  <https://orcid.org/0000-0002-5064-9495>
S. Germani  <https://orcid.org/0000-0002-2233-6811>
F. Giacchino  <https://orcid.org/0000-0002-0247-6884>
N. Giglietto  <https://orcid.org/0000-0002-9021-2888>
M. Giliberti  <https://orcid.org/0009-0007-2835-2963>
F. Giordano  <https://orcid.org/0000-0002-8651-2394>
M. Giroletti  <https://orcid.org/0000-0002-8657-8852>
S. Guiriec  <https://orcid.org/0000-0001-5780-8770>

R. Gupta  <https://orcid.org/0000-0003-4905-7801>
M. Hashizume  <https://orcid.org/0009-0003-4534-9361>
E. Hays  <https://orcid.org/0000-0002-8172-593X>
J. W. Hewitt  <https://orcid.org/0000-0002-4064-6346>
A. Holzmann Airasca  <https://orcid.org/0009-0007-8169-4719>
D. Horan  <https://orcid.org/0000-0001-5574-2579>
X. Hou  <https://orcid.org/0000-0003-0933-6101>
T. Kayanoki  <https://orcid.org/0000-0002-6960-9274>
M. Kuss  <https://orcid.org/0000-0003-1212-9998>
S. Larsson  <https://orcid.org/0000-0003-0716-107X>
A. Laviron  <https://orcid.org/0000-0003-1521-7950>
J. Li  <https://orcid.org/0000-0003-1720-9727>
A. Liguori  <https://orcid.org/0009-0001-4240-6362>
I. Liodakis  <https://orcid.org/0000-0001-9200-4006>
P. Loizzo  <https://orcid.org/0000-0002-2404-760X>
F. Longo  <https://orcid.org/0000-0003-2501-2270>
F. Loparco  <https://orcid.org/0000-0002-1173-5673>
S. López Pérez  <https://orcid.org/0000-0002-2887-4776>
L. Lorusso  <https://orcid.org/0000-0002-2549-4401>
M. N. Lovellette  <https://orcid.org/0000-0002-0332-5113>
P. Lubrano  <https://orcid.org/0000-0003-0221-4806>
S. Maldera  <https://orcid.org/0000-0002-0698-4421>
A. Manfreda  <https://orcid.org/0000-0002-0998-4953>
G. Martí-Devesa  <https://orcid.org/0000-0003-0766-6473>
R. Martinelli  <https://orcid.org/0009-0004-0133-7227>
M. N. Mazziotta  <https://orcid.org/0000-0001-9325-4672>
I. Mereu  <https://orcid.org/0000-0003-0219-4534>
P. F. Michelson  <https://orcid.org/0000-0002-1321-5620>
N. Mirabal  <https://orcid.org/0000-0002-7021-5838>
T. Mizuno  <https://orcid.org/0000-0001-7263-0296>
P. Monti-Guarnieri  <https://orcid.org/0000-0002-1434-1282>
M. E. Monzani  <https://orcid.org/0000-0002-8254-5308>
A. Morselli  <https://orcid.org/0000-0002-7704-9553>
I. V. Moskalenko  <https://orcid.org/0000-0001-6141-458X>
M. Negro  <https://orcid.org/0000-0002-6548-5622>
N. Omodei  <https://orcid.org/0000-0002-5448-7577>
J. F. Ormes  <https://orcid.org/0000-0002-7220-6409>
D. Paneque  <https://orcid.org/0000-0002-2830-0502>
G. Panzarini  <https://orcid.org/0000-0002-2586-1021>
M. Persic  <https://orcid.org/0000-0003-1853-4900>
M. Pesce-Rollins  <https://orcid.org/0000-0003-1790-8018>
V. Petrosian  <https://orcid.org/0000-0002-2670-8942>
R. Pillera  <https://orcid.org/0000-0003-3808-963X>
G. Principe  <https://orcid.org/0000-0003-0406-7387>
S. Rainò  <https://orcid.org/0000-0002-9181-0345>
R. Rando  <https://orcid.org/0000-0001-6992-818X>
B. Rani  <https://orcid.org/0000-0001-5711-084X>
M. Razzano  <https://orcid.org/0000-0003-4825-1629>
A. Reimer  <https://orcid.org/0000-0001-8604-7077>
O. Reimer  <https://orcid.org/0000-0001-6953-1385>
M. Sánchez-Conde  <https://orcid.org/0000-0002-3849-9164>
P. M. Saz Parkinson  <https://orcid.org/0000-0001-6566-1246>
D. Serini  <https://orcid.org/0000-0002-9754-6530>
C. Sgrò  <https://orcid.org/0000-0001-5676-6214>
E. J. Siskind  <https://orcid.org/0000-0002-2872-2553>
P. Spinelli  <https://orcid.org/0000-0001-6688-8864>

D. Tak  <https://orcid.org/0000-0002-9852-2469>
L. Tibaldo  <https://orcid.org/0000-0001-7523-570X>
D. F. Torres  <https://orcid.org/0000-0002-1522-9065>
J. Valverde  <https://orcid.org/0000-0002-8090-6528>
Z. Wadiasingh  <https://orcid.org/0000-0002-9249-0515>

References

- Abdo, A. A., Ackermann, M., Ajello, M., et al. 2011, *ApJ*, 734, 116
Ackermann, M., Ajello, M., Albert, A., et al. 2016, *PhRvD*, 93, 082001
Aguilar, M., Cavasonza, L. A., Ambrosi, G., et al. 2021, *PhRvL*, 127, 271102
Aguilar, M., Cavasonza, L. A., Ambrosi, G., et al. 2023, *PhRvL*, 130, 161001
Albert, A., Alfaro, R., Alvarez, C., et al. 2023, *PhRvL*, 131, 051201
Alexander, T. 2013, arXiv:1302.1508
Atwood, W., Albert, A., Baldini, L., et al. 2013, arXiv:1303.3514
Atwood, W. B., Abdo, A. A., Ackermann, M., et al. 2009, *ApJ*, 697, 1071
Aguilar, M., Cavasonza, L. A., Ambrosi, G., et al. 2018, *PhRvL*, 121, 051102
Ajello, M., Baldini, L., Bastieri, D., et al. 2021, *ApJS*, 252, 13
Arsioli, B., & Orlando, E. 2024, *ApJ*, 962, 52
Aslam, O. P. M., Luo, X., Potgieter, M. S., et al. 2023, *ApJ*, 947, 72
Becker Tjus, J., Desiati, P., Döpper, N., et al. 2020, *A&A*, 633, A83
Blandford, R. D., & McKee, C. F. 1982, *ApJ*, 255, 419B
Bruehl, P., Burnett, T. H., Digel, S. W., et al. 2018, arXiv:1810.11394
Caballero-Lopez, R. A., Engelbrecht, N. E., & Richardson, J. D. 2019, *ApJ*, 883, 73
Edelson, R. A., & Krolik, J. H. 1988, *ApJ*, 333, 646E2
Gleeson, L. J., & Axford, W. I. 1968, *ApJ*, 154, 1011
Gutiérrez, M., & Masip, M. 2020, *Aph*, 119, 102440
Hudson, H. S. 1989, in Proc. Gamma Ray Observatory Workshop (Greenbelt: Goddard Space Flight Center), ed. W. N. Johnson, 4
Hudson, H. S., MacKinnon, A., Szydlarski, M., et al. 2020, *MNRAS*, 491, 4852
Janardhan, P., Fujiki, K., Ingale, M., et al. 2018, *A&A*, 618, A148
Li, J.-T., Beacom, J. F., Griffith, S., et al. 2024, *ApJ*, 961, 167
Li, Z., Ng, K. C. Y., Chen, S., et al. 2024, *ChPhC*, 48, 045101
Linden, T., Beacom, J. F., Peter, A. H. G., et al. 2022, *PhRvD*, 105, 063013
Linden, T., Li, J.-T., Zhou, B., et al. 2025, arXiv:2505.04625
Linden, T., Zhou, B., Beacom, J. F., et al. 2018, *PhRvL*, 121, 131103
Mattox, J. R., Bertsch, D. L., Chiang, J., et al. 1996, *ApJ*, 461, 396
Mazziotta, M. N. 2025, *PhRvD*, 119, 102440
Mazziotta, M. N., Luque, P. D. L. T., Di Venere, L., et al. 2020, *PhRvD*, 101, 083011
Moskalenko, I. V., Porter, T. A., & Digel, S. W. 2006, *ApJL*, 652, L65
Ng, K. C. Y., Beacom, J. F., Peter, A. H. G., et al. 2016, *PhRvD*, 94, 023004
Ng, K. C. Y., Hillier, A., & Ando, S. 2024, arXiv:2405.17549
Niblaeus, C., Beniwal, A., & Edsjö, J. 2019, *JCAP*, 2019, 011
Orlando, E., Petrosian, V., & Strong, A. 2023, *ApJ*, 943, 173
Orlando, E., & Strong, A. 2021, *JCAP*, 04, 004
Orlando, E., & Strong, A. W. 2007, *Ap&SS*, 309, 359
Orlando, E., & Strong, A. W. 2008, *A&A*, 480, 847
Pearson, E. S. 1931, *JASA*, 26, 128
Pearson, E. S. 1932, *JASA*, 27, 424
Pearson, K. F. R. S. 1920, *Biometrika*, 13, 25
Petrosian, V., Orlando, E., & Strong, A. 2023, *ApJ*, 943, 21
Potgieter, M. S. 2013, *LRSP*, 10, 3
Potgieter, M. S., & Vos, E. E. 2017, *A&A*, 601, A23
Puzzoni, E., Frascetti, F., Kóta, J., et al. 2024, *ApJ*, 973, 118
Riechers, P. M., & Crutchfield, J. P. 2021, *PhRvR*, 3, 013170
Scargle, J. D. 2020, *ApJ*, 895, 90
Seckel, D., Stanev, T., & Gaisser, T. K. 1991, *ApJ*, 382, 652
Tang, Q.-W., Ng, K. C. Y., Linden, T., et al. 2018, *PhRvD*, 98, 063019
Thompson, D. J., Bertsch, D. L., Morris, D. J., & Mukherjee, R. 1997, *JGR*, 102, 14735
Tomassetti, N., Bertucci, B., & Fiandrini, E. 2022, *PhRvD*, 106, 103022
Tomassetti, N., Orcinha, M., Barão, F., et al. 2017, *ApJL*, 849, L32
Upton, L. A., & Hathaway, D. H. 2023, *JGRA*, 128, e2023JA031681
Yule, G. U. 1926, *JRSSD*, 19, 1
Zhou, B., Ng, K. C. Y., Beacom, J. F., et al. 2017, *PhRvD*, 96, 023015